Two-Dimensional Contribution Map for Fault Identification

XIAOXIANG ZHU and RICHARD D. BRAATZ

All control engineers should be able to detect and identify faults (that is, abnormal conditions in a system) from the analysis of large heterogeneous time-series data sets. This "Focus on Education" column provides an introduction to multivariable data-based methods for fault detection and fault identification, with the latter being the determination of system variables that contribute the most to a detected fault. For fault identification in statistical process monitoring, the contribution plot is the most commonly used tool for quickly identifying the most affected variables. Contribution calculations are revisited in the context of principal component analysis (PCA) and T^2 statistics, and a two-dimensional (2-D) contribution map is illustrated for the examination of time-series data under faulty conditions. The 2-D contribution map is compared to the traditional one-dimensional (1-D) contribution plot using simulated data from a realistic chemical process. The 2-D contribution map demonstrates the potential to enable a greater understanding of the fault and how its effects are propagated through the system.

INTRODUCTION

Faults inevitably occur in industrial systems and become more prevalent as systems become increasingly large scale and interconnected. The closed-loop performance of the control system depends critically on the proper functioning of the process and control equipment, so faults need to be detected and diagnosed quickly from the real-time data collected from the system. Rapid detection and diagnosis can minimize downtime, increase the safety of plant operations, and reduce manufacturing costs. Statistical process monitoring (SPM) applies multivariate data-driven methods to process data for fault detection and diagnosis and has been popular in both academic research and industrial practice over the past two decades [1]–[5]. Data-driven methods such as PCA, partial least squares (PLS), and other modified methods are used to characterize the data collected during normal process conditions. Such methods are dimensionality reduction techniques that project the high-dimensional process data into much lower dimensional spaces. Fault detection is based on multivariate statistics, such as T^2 statistics for describing variations within the lower dimensional space and Q statistics for representing variations in the residual space, in which rigorously derived control limits are computed from the data [1]–[5].

Typical procedures in SPM involve a fault identification step after the detection of a fault to identify the most likely variables closely associated with the fault (that is, the "faulty variables") by analyzing each variable's contributions [4]. A contribution plot summarizes quantitative information about the potentially faulty variables. While useful, the traditional contribution plot only examines the contributions at one observation (time point), and multiple contribution plots are needed to illustrate multiple observations in time series data. In comparison, a 2-D contribution map stacks multiple observations into one image to clearly illustrate the contribution of the variables over the entire faulty data times series, which enables the fast identification of faulty variables within large heterogeneous data sets.

The next section is an introduction to PCA [1]–[5], which is the most commonly used technique for fault detection and identification for large heterogeneous data sets. The 2-D contribution map is presented as a more effective visualization than the commonly used 1-D contribution plot used for fault identification. The methods are illustrated and compared through application to data collected from a well-known model problem known as the Tennessee Eastman process (TEP).

PCA AND T^2 STATISTIC REVISITED

Consider a data matrix $X \in \mathcal{R}^{m\times n}$ containing m observations of n process variables at the normal process conditions. The matrix X should be *autoscaled*, that is, each process variable should be pretreated by subtracting its mean and dividing by its standard deviation. PCA dimensionality reduction uses the singular value decomposition

$$\frac{1}{\sqrt{m-1}}X = U\Sigma V^{\mathrm{T}}, \tag{1}$$

where $U \in \mathcal{R}^{m\times m}$ and $V \in \mathcal{R}^{n\times n}$ are unitary matrices and $\Sigma \in \mathcal{R}^{m\times n}$ is a diagonal matrix containing the singular values in decreasing order $(\sigma_1 \geq \sigma_2 \geq \cdots \geq \sigma_{\min\{m,n\}} \geq 0)$.

For each principal component i, its *loading vector* is given by the ith column vector of the matrix V, with the variance of the projected training data along the loading vector being equal to σ_i^2.

In the data-modeling step, only a small number of the principal components, known as the *reduction order* a, are

Digital Object Identifier 10.1109/MCS.2014.2333295
Date of publication: 16 September 2014

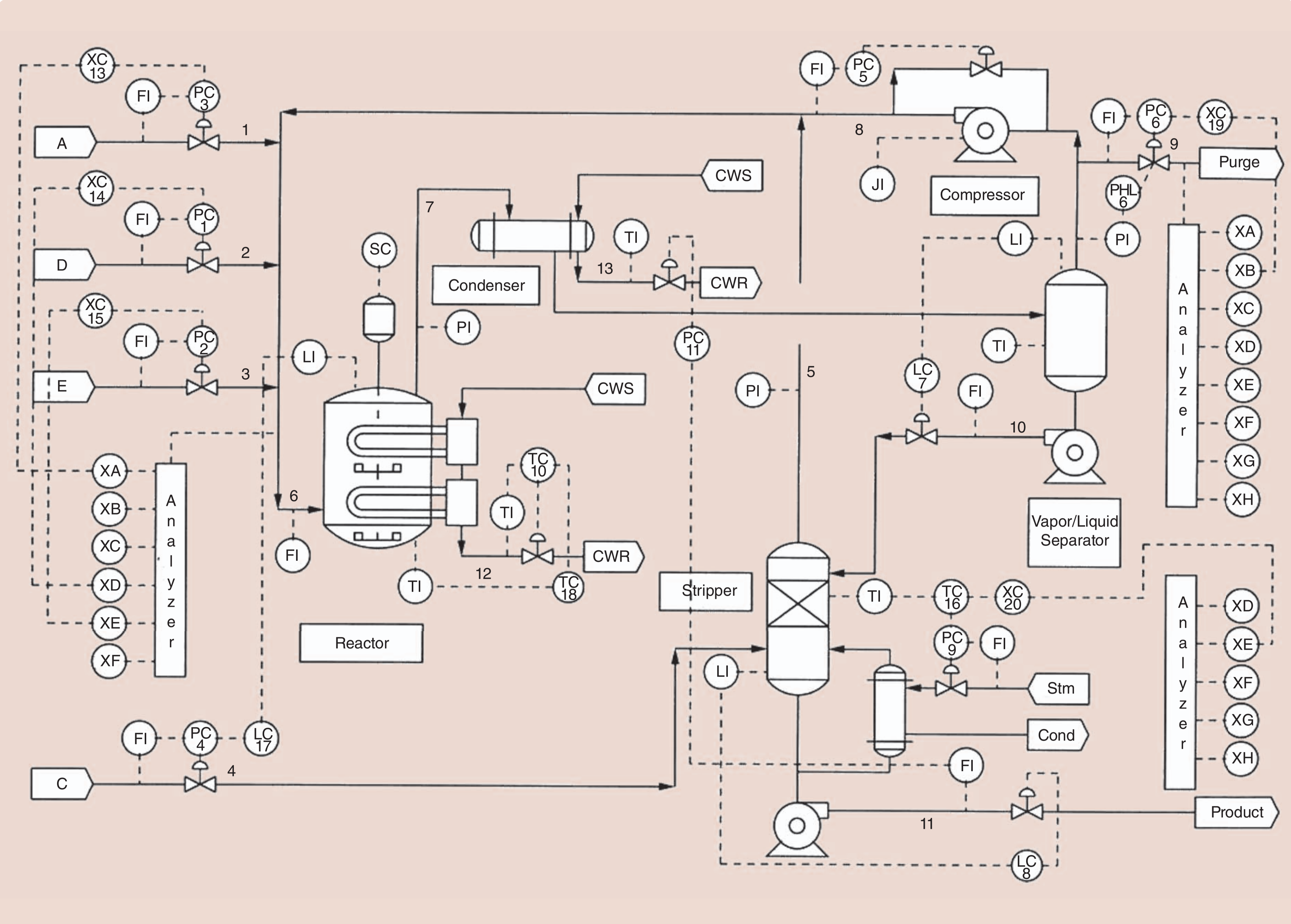

FIGURE 1 The Tennesse Eastman process flow diagram with plant-wide control structure [2], [9].

retained in the PCA model. Several methods are available for determining the value of a, including the percent variance test, the scree test, and cross validation [1]–[5]. For demonstration purposes, this article uses the percentage variance test, which chooses a based on the lower dimensional space containing a specified minimum percentage of the total variance (for example, at least 95%).

Once the reduction order a is determined, the *loading matrix* $P \in \mathcal{R}^{n \times a}$ is the first a column vectors in the V matrix.

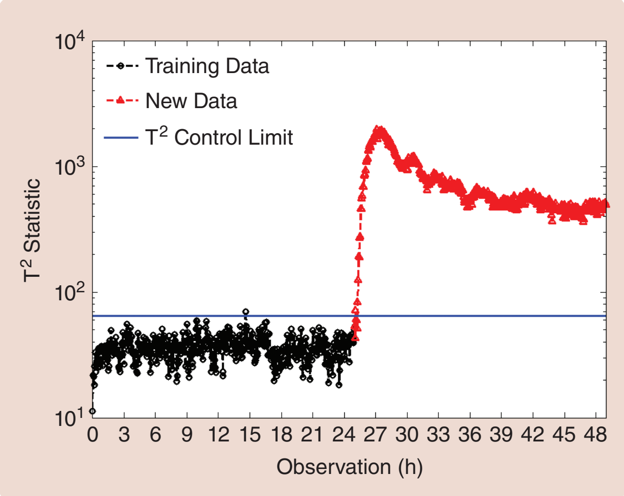

FIGURE 2 The T^2 statistic for normal training data (black) and faulty test data (red) indicates that Fault #1 is detected after hour 25.

For an observation $x \in \mathcal{R}^{n \times 1}$, the *score vector* $\boldsymbol{t}$, which represents the data projection onto the principal components, is

$$t = P^T x. \tag{2}$$

The T^2 statistic, which is a measure of how far the observation is from the center of the characterized normal data, can be calculated directly from the PCA representation by

$$T^2 = x^T P \Sigma_a^{-2} P^T x, \tag{3}$$

where $\Sigma_a \in \mathcal{R}^{a \times a}$ is a diagonal matrix containing the first a rows and columns of Σ in (1).

The threshold for detecting abnormalities in new observations is given by the T^2 statistic

$$T^2_{\mathrm{CL}}(\alpha) = \frac{a(m-1)(m+1)}{m(m-a)} F_\alpha(a, m-a), \tag{4}$$

where $F_\alpha(a, m-a)$ defines the upper $100\alpha\%$ critical point of the F-distribution with a and $m-a$ degrees of freedom. When the T^2 statistics of the new observations (for example, two consecutive observations) violate the threshold, a fault is alarmed.

Fault identification is carried out immediately after a fault is detected in the process data using the T^2 or any alternative fault detection statistic. The *contribution plot* quantifies the contribution of each process variable to the PCA scores (2) to identify the process variables that are most closely associated with, and potentially responsible for or a direct consequence of, the abnormal/out-of-control status. The procedure for the calculation of the contributions is [4]:

1) Given a vector of observations $\boldsymbol{x}$ (auto-scaled with the mean and variance of the training data) and its calculated score vector $\boldsymbol{t}$, the *contribution* of each process variable x_j to each t_i in the score vector $\boldsymbol{t}$ is calculated from

$$\mathrm{cont}(i,j) = \begin{cases} \dfrac{t_i}{\sigma_i^2} P_{j,i} x_j & \text{if } \dfrac{t_i}{\sigma_i^2} P_{j,i} x_j \geq 0 \\ 0 & \text{if } \dfrac{t_i}{\sigma_i^2} P_{j,i} x_j < 0 \end{cases} \tag{5}$$

where $P_{j,i}$ is the (j,i)th element of the loading matrix P.

2) The *total contribution* of the process variable j at the observation is calculated by

$$\mathrm{CONT}(j) = \sum_{i=1}^{a} \mathrm{cont}(i,j). \tag{6}$$

For each observation, the CONT is a vector whose length is equal to the number of process variables. In

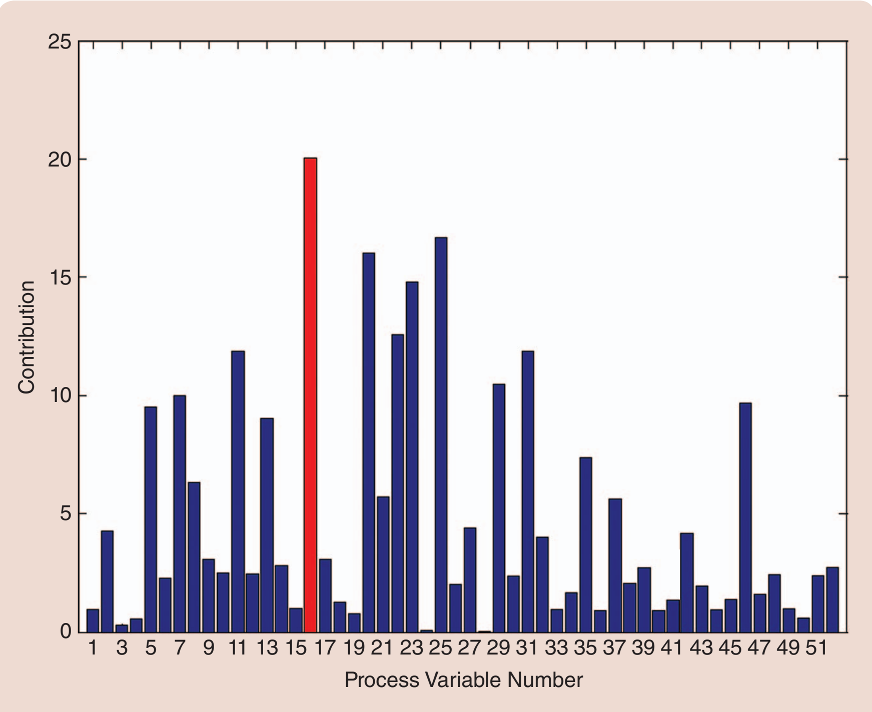

FIGURE 3 A traditional contribution plot of the testing data set at the time of the detection of Fault #1.

the traditional contribution plot, the CONT is plotted for the observation at which the fault is detected. For time-series data, the procedure is repeated to generate one contribution plot at each observation. A 2-D contribution map, which stacks the series of observations in one single color map, is a more convenient alternative for representing the information. The usefulness of the 2-D contribution map is illustrated in the next section.

TENNESSEE EASTMAN PROCESS EXAMPLE

The TEP is a realistic simulation of a chemical facility created by the Tennessee Eastman Company [6]. The TEP is widely used by researchers for evaluating process control and monitoring methods (see, for example, [2], [7], and [8]). Figure 1 shows the TEP flow diagram with a plant-wide control structure, which has 41 measurements, 12 manipulated variables, and 21 preprogrammed faults. The process consists of three main units (a reactor, a separator, and a stripper), and produces two products (labeled G and H) from four reactants (labeled A, C, D, and E). The process is nonlinear, open-loop unstable, and contains a mixture of fast and slow dynamics. The closed-loop system is stable and provided acceptable performance over the entire operating regime when no faults occur in the system. Of the 21 preprogrammed faults, some faults are detectable and identifiable using classical single-variable control charts such as Shewhart, exponentially weighted moving average (EWMA), and cumulative sum (CUSUM) whereas some faults are challenging for even the most advanced methods. Detailed descriptions of the process and the control structure, as well as a description of the classical control charts, are available in [2] and [9].

In this example, the data under the normal operating conditions were used as the training data for PCA modeling, and the data collected during Fault #1 was used as the testing data for demonstrating the method (the data are available online at http://web.mit.edu/braatzgroup/TE_process.zip). Fault #1 is a step change in the A/C feed

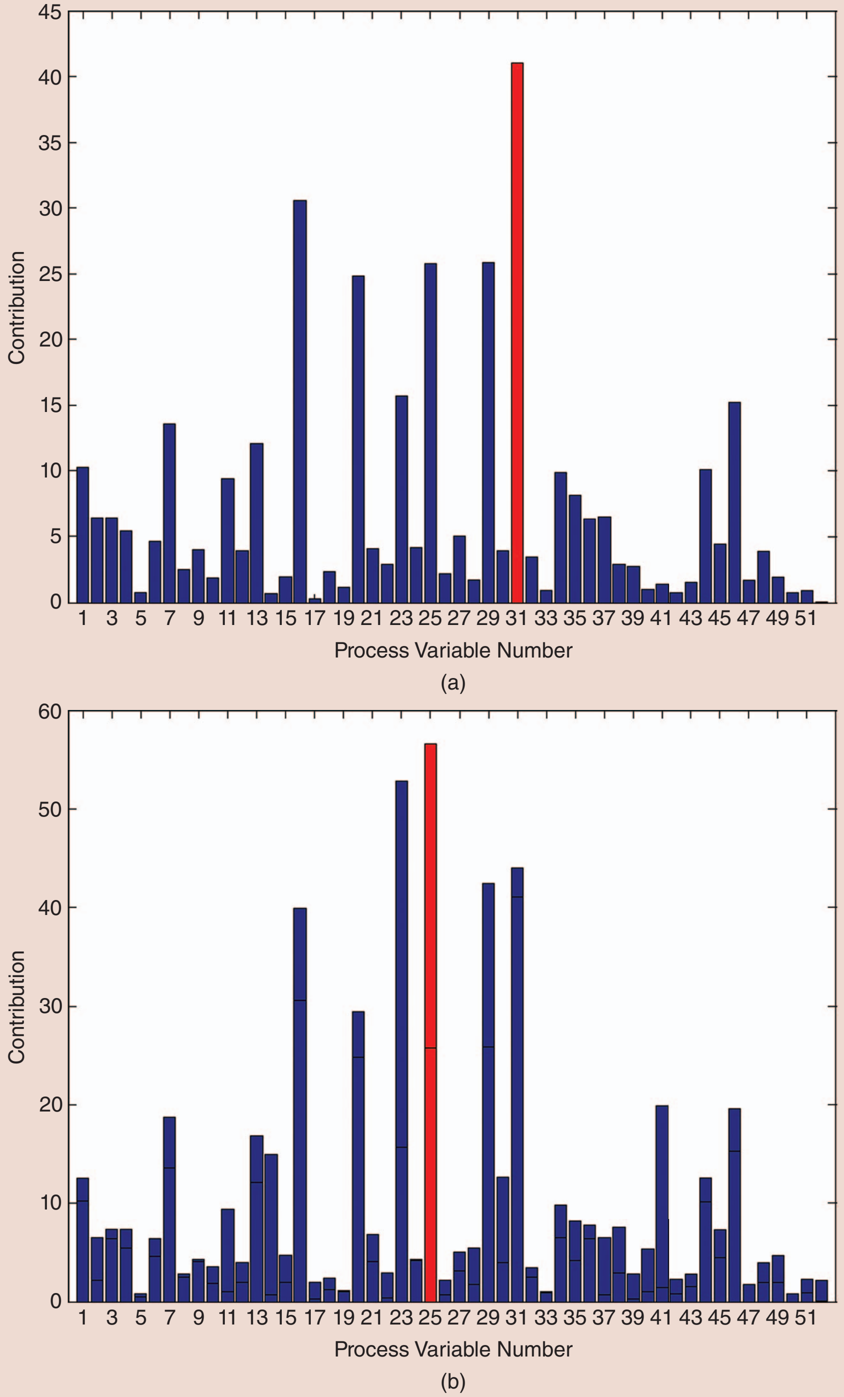

FIGURE 4 Different most-faulty variables were picked out in the traditional contribution plot. (a) One and (b) three samples after the time of the detection of Fault #1.

TABLE 1 Pseudocode for implementation of the 2-D contribution map.

```
% pretreat the testing data (auto-scaling)
X = pretreat(X);
% calculate the contributions
[m,n] = size(X);
CONT = zeros (m,n);
for k = 1:m            % for each new observation k
  t = P' * X(k,:)';
  cont = zeros(a, n)
  for i = 1:a          % for each principal component
    for j = 1:n        % for each process variable
        cont(i,j) = t(i) * X(k,j) * P(i, j)/σ_i^2;
        cont(i,j) = cont(i, j) * (cont(i, j) > 0);
    end
  end
  CONT(k,:) =sum(cont, 1);
end
% plot the 2-D contribution map
imagesc(CONT');
x label('New Observations (hour)');
y label('Process Variable');
```

ratio in Stream 4 (Figure 1). The data set for normal operating conditions contains 500 observations equally sampled over 25 h, and the data set for Fault #1 has 480 observations equally sampled during a 24-h period. Based on the normal training data, a reduction order $a = 36$ was obtained to retain 95% of the variance. Figure 2, which shows the T^2 statistic of the training and testing data sets, indicates a fault detected at around hour 25, several sample times after the fault has occurred. The control limit shown as a blue line was calculated by (4) at the 99% confidence level.

The traditional contribution plot in Figure 3 illustrates the contribution of process variables at the observation upon which the fault was detected (the fault was alarmed after two consecutive T^2 control limit violations or eight sampling points after the fault occurrence). The plot suggests the fault is most likely associated with process variable 16 (XMEAS 16, the stripper pressure). However, contribution plots for subsequent observations show different variables having the largest contributions (Figure 4). In this circumstance, because of the dynamics of the closed-loop system, the most critical process variables associated with the fault was indeterminate using the 1-D contribution plots.

The same contribution data plotted as the 2-D contribution map in Figure 5 enables the reliable identification of the key process variables associated with the fault: XMEAS 1 (A feed, Stream 1) and XMV 3 (A feed flow, Stream 1), both of which show consistent strong bands of contribution. Fault #1 is involved with a feed ratio change of A/C in Stream 4, and a control loop changed the A feed in Stream 1 to compensate for the fault. The 2-D contribution map indicates low initial contributions of all process variables at times right after the fault occurs and how the effects of the fault are gradually propagated into XMEAS 1 and XMV 3.

Figure 5 shows that in the first few hours following the fault occurrence (hours 25–29), more than a dozen process variables show high contributions to the fault, which corresponds to the period when the closed-loop control system is trying to compensate for the fault. It is unlikely that a control engineer applying 1-D contribution plots to observations in this time period will correctly determine the key faulty variables.

An inspection of Figure 5 indicates that the 1-D contribution plot would correctly identify the variables associated with Fault #1 if the contributions were averaged over 2 h or the data were averaged over two hours before applying the 1-D contribution plot. Averaging over long time windows, however, would directly conflict with the goal of correctly identifying the associated faulty variables quickly after the fault is detected. Further, plotting multiple time series, as in the 2-D contribution map, is generally more useful than plotting single snapshots as done in the 1-D contribution plot because the best time period for identifying faults is not known a priori and will vary depending on the different fault dynamics.

The 1-D contribution plot will typically give comparable results when the fault response is fast and localized. For example, consider Fault #4, which is a change in reactor cooling water inlet temperature. The effect of this fault on the variables is simple enough that the contribution is concentrated on XMV 10 (reactor cooling water flow) from the point of fault occurrence, as shown in Figure 6, so the 1-D contribution plot can also quickly identify the faulty variable.

The 2-D contribution map and the 1-D contribution plot are essentially two ways of presenting the same data. In fact, in Figure 5, each column corresponds to the 1-D contribution plot at that observation time. The 2-D contribution map, however, assembles the information to enable a more useful visualization for identifying the faulty variables. The 2-D contribution map enables the human operators or control engineers to be better informed, to speed their ability to track down the precise nature and cause of the fault.

The implementation of the 2-D contribution map is briefly summarized by the pseudocode in Table 1.

FINAL REMARKS

The 2-D contribution map provides an alternative means of plotting fault contributions compared to the 1-D contribution plot. By plotting multiple observations (time-series data) on the same map, control engineers can more accurately identify the most impacted variables directly and potentially gain a better understanding of the fault and how its effects are propagated through the system.

There are alternative means for calculating the contributions [5]. While the details of the formulas may be different, the idea of the 2-D contribution map is universally applicable. Complementary to the T^2 statistic, the Q statistic, which captures faults in the residual space corresponding to the $m-a$ smallest singular values, can also employ the contribution map for fault identification in a similar manner.

It is the authors' opinion that every control engineer should receive some training in fault detection and diagnosis and that the multivariable statistical methods, as well as classical Shewhart, EWMA, and CUSUM control charts, should be the covered at a minimum. Preferably, this content is contained in a course devoted to the topic of fault detection and diagnosis, which should be a component of any undergraduate or graduate control curriculum. If such a course is not offered, then the content should be covered in one to two lectures of an introductory controls, systems engineering, or data analysis course. At the authors' institution, this material is covered in the modeling and data analysis section of an introductory systems engineering course mostly taken by first-year graduate students.

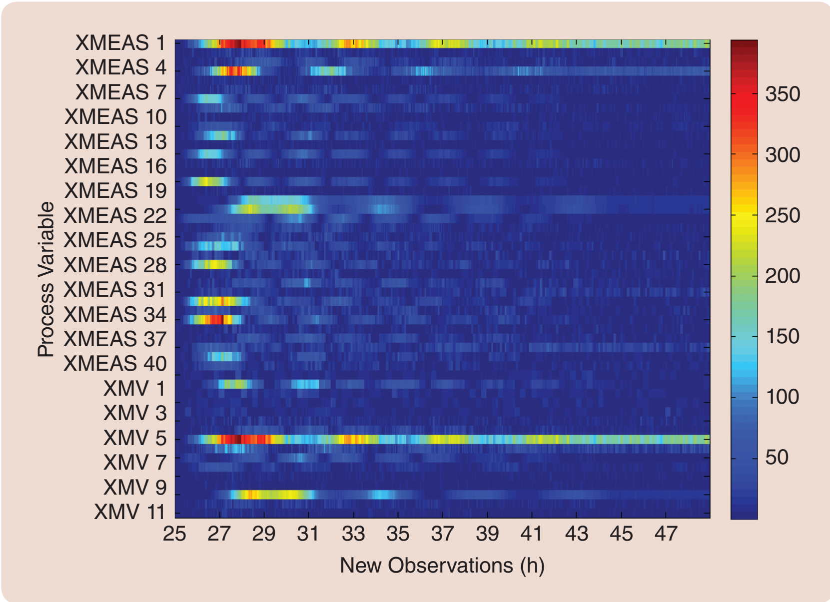

FIGURE 5 A 2-D contribution map of the testing data (Fault #1) provides a visual identification of the most contributing variables in bright bands.

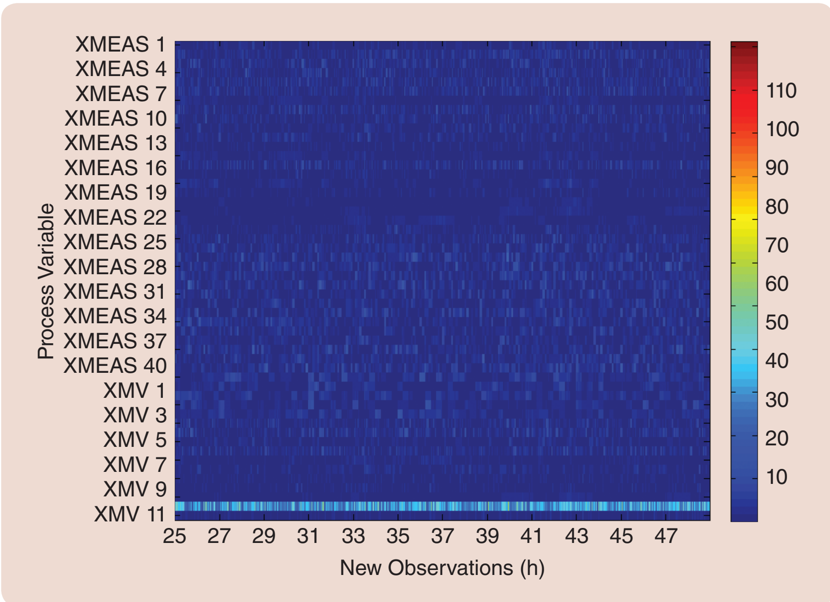

FIGURE 6 A 2-D contribution map for Fault #4.

ACKNOWLEDGMENTS

The authors gratefully acknowledge BP for funding.

REFERENCES

[1] S. J. Qin, "Survey on data-driven industrial process monitoring and diagnosis," *Annu. Rev. Contr.*, vol. 36, no. 2, pp. 220–234, 2012.

[2] L. H. Chiang, E. L. Russell, and R. D. Braatz, *Data-Driven Methods for Fault Detection and Diagnosis in Industrial Systems*. London: Springer-Verlag, 2000.

[3] S. J. Qin, "Statistical process monitoring: Basics and beyond," *J. Chemomet.*, vol. 17, nos. 8–9, pp. 480–502, 2003.

[4] J. A. Westerhuis, S. P. Gurden, and A. K. Smilde, "Generalized contribution plots in multivariate statistical process monitoring," *Chemomet. Intell. Lab. Syst.*, vol. 51, no. 1, pp. 95–114, 2000.

[5] T. Kourti and J. F. MacGregor, "Multivariate SPC methods for process and product monitoring," *J. Qual. Technol.*, vol. 28, no. 4, pp. 409–428, 1996.

[6] J. J. Downs and E. F. Vogel, "A plant-wide industrial process control problem," *Comput. Chem. Eng.*, vol. 17, no. 3, pp. 245–255, 1993.

[7] N. L. Ricker and J. H. Lee, "Nonlinear model predictive control of the Tennessee Eastman challenge process," *Comput. Chem. Eng.*, vol. 19, no. 9, pp. 961–981, 1995.

[8] T. J. McAvoy and N. Ye, "Base control for the Tennessee Eastman problem," *Comput. Chem. Eng.*, vol. 18, no. 5, pp. 383–413, 1994.

[9] P. R. Lyman and C. Georgakis, "Plant-wide control of the Tennessee Eastman problem," *Comput. Chem. Eng.*, vol. 19, no. 3, pp. 321–331, 1995.